J. Opt. B: Quantum Semiclass. Opt. **1** (1999) 101–106. Printed in the UK PII: S1464-4266(99)95985-2

# Numerical investigation of laser localized structures

**A G Vladimirov†§, S V Fedorov‡, N A Kaliteevskii‡, G V Khodova‡ and N N Rosanov‡‖**

† St Petersburg State University, Physics Faculty, 1 Ulianovskaya st, 198904 St Petersburg, Russia
‡ Institute for Laser Physics, Vavilov State Optical Institute, Birzhevaya line 12, 199034 St Petersburg, Russia

Received 29 June 1998, in final form 12 November 1998

**Abstract.** We study stability and bifurcations of 1D localized structures in a laser with a saturable absorber. Instability leading to oscillating localized structure is described. Our numerical study of light propagation in a dispersive medium with saturable gain and absorption provides evidence for the existence of 3D 'laser bullets'.

**Keywords:** Dissipative localized structures, laser with saturable absorption, bifurcations, stability, laser bullets

## 1. Introduction

The term 'localized structures (LSs) of laser radiation' is used for structures formed in a limited region of the transverse section of laser systems, for example, in wide-aperture lasers. They are of particular interest since they represent the case of self-organization in nonlinear coherent optical systems and have promising applications in optical data processing. Stable localized laser structures, 'laser autosolitons', were first predicted in [1] and were investigated theoretically in [2–5] (see also the literature cited there). Recently, such structures were observed experimentally in a cavity with photorefractive crystals serving as the gain and loss elements [6, 7] and in a dye laser with bacteriorhodopsin as a saturable absorber [8]. Mathematical aspects of a theory of similar structures were studied without specific reference to lasers (see [9, 10] and the references therein). Laser autosolitons representing islands of lasing against the background of a stable nonlasing regime and formed by hard excitation, are very similar to localized structures in bistable passive nonlinear optical systems, such as wide-aperture nonlinear interferometers excited by external radiation investigated earlier. Stationary and pulsating 'diffraction autosolitons' arising in driven passive optical devices were predicted theoretically [11, 12] and detected experimentally [13, 14] (see also the review [3]). 'Diffusive autosolitons' were investigated intensively earlier in various physical, chemical and biological systems [15, 16].

Here we study stability and bifurcations of 1D localized solutions arising in a model of a wide-aperture laser with a saturable absorber. Numerical evidence for the existence of 3D 'laser bullets' arising in a medium with saturable gain, absorption and frequency dispersion is presented.

§ E-mail address: `andrei@snp.usr.pu.ru`
‖ E-mail address: `rosanov@ilph.spb.su`

## 2. Laser model

We start with the consideration of 1D localized structures arising in transverse section of a wide aperture bistable ring laser with a saturable absorber. The laser model is described by the equation governing the evolution of the dimensionless complex electric field envelope $E$ [3, 4]

$$\partial_t E = \mathrm{i}\partial_{xx} E + E f(|E|^2), \qquad (1)$$

where

$$f(|E|^2) = -1 + \frac{\mathcal{L}_1(1-\mathrm{i}\Delta_1)g_0}{1+\mathcal{L}_1|E|^2/\beta} - \frac{\mathcal{L}_2(1-\mathrm{i}\Delta_2)a_0}{1+\mathcal{L}_2|E|^2}. \qquad (2)$$

The time $t$ is normalized by the cavity relaxation rate; $x$ is the dimensionless transverse coordinate. The parameters $g_0$ and $a_0$ describe linear gain and linear absorption, respectively; $\beta = I_g/I_a$ is the ratio of the saturation intensities. The parameter $\Delta_1$ ($\Delta_2$) describes frequency detuning between cavity eigenfrequency and amplification (absorption) line centre; $\mathcal{L}_{1,2} = (1+\Delta_{1,2}^2)^{-1}$. Spatially homogeneous dynamical regimes arising in a detuned laser with a saturable absorber are described in [17]. Note, that after the substitution $t \to z$, $x \to t$ equation (1) is transformed into the simplest equation describing light propagation in a single mode fibre with saturable amplification and absorption [3]. Here $z$ is the coordinate along the fibre axis.

Equation (1) is invariant under phase shift of the electric field envelope and under translations in space. These symmetry properties are defined by the transformations

$$E(x,t) \to E(x,t)\mathrm{e}^{\mathrm{i}\eta}, \qquad (3)$$

$$E(x,t) \to E(x+h,t), \qquad (4)$$

with arbitrary $\eta$ and $h$. They are preserved in the case of finite population relaxation rates in amplifying and absorbing media. In addition, equation (1) describing a laser with inertionless media is invariant under 'Galilean transformation' (transformation to a moving system of coordinates):

$$E(x,t) \to E(x - vt, t)\mathrm{e}^{\mathrm{i}vx/2 - \mathrm{i}v^2 t/4}. \qquad (5)$$

This means that any motionless solution of equation (1) generates a family of uniformly moving solutions each characterized by some definite value of the velocity $v$. For finite values of the population relaxation rates 'Galilean transformation' symmetry is broken and, hence, localized structures cannot travel with arbitrary constant velocity. In this case uniformly moving autosolitons are expected to have some fixed velocity.

## 3. Localized solutions

Let us consider the stationary motionless localized solution of equation (1) which is characterized by the time independent transverse distribution of the laser intensity $|E|^2 = I(x)$:

$$E = A(x)\mathrm{e}^{-\mathrm{i}\alpha t}, \qquad (6)$$

with $A(x) \to 0$ for $x \to \pm\infty$. Substituting (6) into (1) we get the ordinary differential equation for the autosoliton amplitude

$$\partial_{xx} A + \alpha A - \mathrm{i}Af(|A|^2) = 0, \qquad (7)$$

with $f(|A|^2)$ defined by equation (2). Here the values of the spectral parameter $\alpha$ (frequency shift of the laser field) for which stationary localized solutions exist, are to be determined. After the substitution $A(x) = a(x)\mathrm{e}^{\mathrm{i}\Phi(x)}$, equation (7) can be rewritten in the form [5, 10]

$$\begin{gathered} \partial_x a = ak \qquad \partial_x q = -2qk + \mathrm{Re}\, f(a^2) \\ \partial_x k = -\alpha + q^2 - k^2 - \mathrm{Im}\, f(a^2), \end{gathered} \qquad (8)$$

where $q = \partial_x \Phi$ and $k = a^{-1}\partial_x a$. Equations (8) possess two steady-state solutions which correspond to zero laser-field intensity

$$\begin{gathered} \mathrm{L}_\pm : a = 0 \\ q_\pm = \pm(\tfrac{1}{2}[(\alpha + f_{02})^2 + {f_{01}}^2]^{1/2} + \alpha + f_{02})^{1/2} \\ k_\pm = f_{01}/2q_\pm . \end{gathered} \qquad (9)$$

Here $f_{01} = \mathrm{Re}\, f(0) = -1 + g_0 - a_0$ and $f_{02} = \mathrm{Im}\, f(0) = -(g_0\Delta_1 - a_0\Delta_2)$. Each of the steady states (9) has a single real eigenvalue and a pair of complex conjugated eigenvalues defined by $\lambda_1^\pm = k_\pm$, $\lambda_2^\pm = -2(k_\pm + \mathrm{i}q_\pm)$, and $\lambda_3^\pm = \lambda_2^{\pm *}$. Since in the bistability domain we have $f_{01} < 0$, $\mathrm{L}_-$ ($\mathrm{L}_+$) is a saddle focus with 1D unstable (stable) manifold and 2D stable (unstable) manifold. Stationary LS corresponds to heteroclinic trajectory of equations (8) connecting the fixed points $\mathrm{L}_-$ and $\mathrm{L}_+$. Thus, the process of finding stationary LS includes identifying the bifurcation points in the parameter space for which equations (8) have a heteroclinic trajectory of the type described. Specifically, the single-humped 'one-soliton' solution corresponds to the simplest ('single-pass') heteroclinic orbit that visits vicinities of the fixed points $\mathrm{L}_-$ to $\mathrm{L}_+$ only once. As was shown in [5], the existence of such LS implies the existence of an infinite number of multi-humped solutions that can be considered as stationary LSs formed by two or more coupled 'one-soliton' solutions. Moreover, for any given $n$ there exists an infinite countable number of $n$-humped solutions differing by the distances between coupled 'one-soliton' solutions.

Due to the symmetry property $x \to -x$ of equations (1) the equations (8) are invariant under the transformation $(x, a, q, k) \to (-x, a, -q, -k)$. Using this fact and that for given laser parameter values there can exist only one heteroclinic trajectory connecting the steady states $\mathrm{L}_\pm$ one can easily show that any LS associated with the heteroclinic orbit of equations (8) can be described (after an appropriate shift of the reference point for the coordinate $x$) by an even function $A(x) = A(-x)$. It follows that in the phase space of equations (8) the midpoint of the heteroclinic trajectory corresponding to the symmetry centre of the even LS ($x = 0$) lies on the $a$-axis ($q = k = 0$). Therefore, in order to find the spectral parameter value for which equations (8) have a heteroclinic solution we can use the following procedure. First we calculate the intersection point $(a_0, 0, k_0)$ of the 1D unstable manifold of the fixed point $\mathrm{L}_-$ with the 2D plane $q = 0$. Then we find the value of the parameter $\alpha$ for which the intersection point hits the $a$-axis ($k_0 = 0$). This procedure serves as a basis for an effective numerical procedure of finding stationary localized solutions. Note, that apart from even localized solutions $A(x) = A(-x)$ equation (1) possess odd localized solutions with $A(x) = -A(-x)$ and $A(0) = 0$. Each of them can be associated with a pair of 'solitons' coupled in antiphase. However, since for $A = 0$ the variable $k$ is singular, odd localized solutions cannot be described with the help of equations (8) and require separate consideration [5].

The dependence of the spectral parameter $\alpha$ of the 'one-soliton' solution on the linear gain parameter $g_0$ is presented in figure 1. The curve shown in figure 1 forms an infinite spiral with the end at point P corresponding to a codimension-two heteroclinic bifurcation of equations (8). At this point there exists a heteroclinic connection $\mathrm{L}_- \to \mathrm{N}_- \to \mathrm{N}_+ \to \mathrm{L}_+$, where $\mathrm{N}_-$ and $\mathrm{N}_+$ denote the two of the four fixed points of the system (8) which correspond to nonzero laser intensity. Like $\mathrm{L}_-$ and $\mathrm{L}_+$, these two fixed points are transformed into each other after the transformation $(a, q, k) \to (a, -q, -k)$. Figure 2 represents four different 'one-soliton' solutions existing for the same laser parameter values. In figure 1 these solutions correspond to the intersection points of the 'one-soliton' curve with the dashed vertical line defined by the relation $g_0 = 2.102$. Note, that the only stable solution is the one corresponding to curve 4 in figure 2.

## 4. Autosoliton stability and bifurcations

Let $E(x,t) = A_0(x)\mathrm{e}^{-\mathrm{i}\alpha_0 t}$ be a motionless localized solution of equation (1). Substituting a slightly perturbed autosoliton solution

$$\begin{gathered} E = [\boldsymbol{V}_0(x) + \delta\boldsymbol{V}(\boldsymbol{x})\mathrm{e}^{\lambda t}]\mathrm{e}^{-\mathrm{i}\alpha_0 t} \\ \boldsymbol{V}_0 = (\mathrm{Re}\, A_0, \mathrm{Im}\, A_0)^T \\ \delta\boldsymbol{V} = (\mathrm{Re}\, \delta A, \mathrm{Im}\, \delta A)^T, \end{gathered} \qquad (10)$$

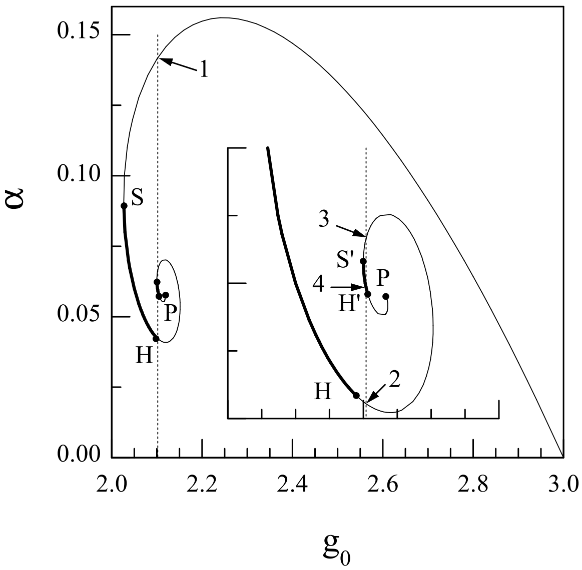


**Figure 1.** Spectral parameter $\alpha$ for the 'one-soliton' solution of equation (1) versus linear gain parameter $g_0$. $a_0 = 2$, $\beta = 10$, and $\Delta_{1,2} = 0$. The inset shows the vicinity of the point P on an enlarged scale. The thick (thin) curve corresponds to the stable (unstable) autosoliton solution. S and S′ (H and H′) are the points of a saddle-node (Andronov–Hopf) bifurcation. P is the codimension-two global bifurcation point for equations (8). The vertical dashed line is defined by $g_0 = 2.102$. Intersections of this line with the 'one-soliton' solution curve are labelled by 1–4. These intersections correspond to the localized solutions shown in figure 2.

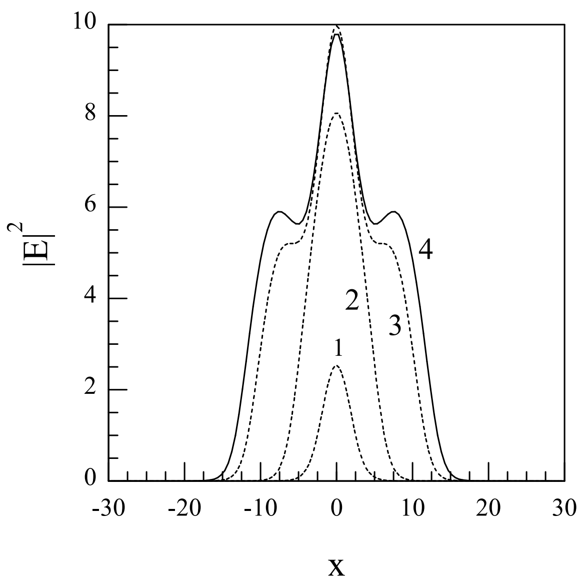


**Figure 2.** Spatial distributions of laser intensity corresponding to four localized structures calculated for $g_0 = 2.102$, $a_0 = 2$, $\beta = 10$, $\Delta_{1,2} = 0$. (1) $\alpha = 0.141\,75$; (2) $\alpha = 0.042\,18$; (3) $\alpha = 0.066\,63$; (4) $\alpha = 0.059\,34$. The only stable solution is the one represented by the solid curve 4.

into the real and imaginary part of equation (1) we get the linear equation $\hat{L}_0 \delta \boldsymbol{V}(x) = \lambda \delta \boldsymbol{V}(x)$, for the eigenvalues $\lambda$ determining the stability of the localized solution. Here the linear operator $\hat{L}_0$ is defined by

$$\hat{L}_0 = \begin{pmatrix} \operatorname{Re} F_+(A_0, A_0^*) & -\alpha_0 - \partial_{xx} - \operatorname{Im} F_-(A_0, A_0^*) \\ \alpha_0 + \partial_{xx} + \operatorname{Im} F_+(A_0, A_0^*) & \operatorname{Re} F_-(A_0, A_0^*), \end{pmatrix} \quad (11)$$

with $F_\pm(A_0, A_0^*) = f(I_0) + f'(I_0)(I_0 \pm A_0^2)$, $I_0 = |A_0|^2$, and $f'(I_0) = (\mathrm{d}f(I)/\mathrm{d}I)_{I=I_0}$. In the bistability domain where the nonlasing solution is stable, the continuous spectrum of the operator (11) lies in the left half-plane of the complex plane and does not produce instability. Therefore, we focus our consideration on the discrete spectrum.

Due to the symmetry properties (3)–(5) the operator (11) has a triply degenerate zero eigenvalue. This eigenvalue corresponds to the eigenvectors

$$\boldsymbol{\Psi}_{1,2}(x) = (\operatorname{Re}\psi_{1,2}, \operatorname{Im}\psi_{1,2})^T, \qquad \psi_1 = \mathrm{i}A_0 \qquad \psi_2 = \partial_x A_0, \quad (12)$$

for which we have $\hat{L}_0 \boldsymbol{\Psi}_{1,2}(x) = 0$. The symmetry property (5) implies that apart from the two eigenvectors $\boldsymbol{\Psi}_{1,2}(x)$ there exists an adjoint vector defined by

$$\boldsymbol{\Psi}_3(x) = (\operatorname{Re}\psi_3, \operatorname{Im}\psi_3)^T, \qquad \psi_3 = -\mathrm{i}xA_0/2. \quad (13)$$

This vector obeys the equation $\hat{L}_0 \boldsymbol{\Psi}_3(x) = \boldsymbol{\Psi}_2(x)$. Note, that since the amplitude $A_0(x)$ of the motionless LS can be taken as either an even or odd function of $x$, the two neutral modes $\boldsymbol{\Psi}_1(x)$ and $\boldsymbol{\Psi}_2(x)$ have opposite parity. Specifically, the 'one-soliton' solution (after an appropriate shift along the $x$-axis) can be described by an even function $A_0(x) = A_0(-x)$ and, therefore, in this case we have $\boldsymbol{\Psi}_1(x) = \boldsymbol{\Psi}_1(-x)$ and $\boldsymbol{\Psi}_2(x) = -\boldsymbol{\Psi}_2(-x)$. Moreover, since for $A_0(x) = A_0(-x)$ we have $\hat{L}_0(x) = \hat{L}_0(-x)$, any eigenvector of the linear operator $\hat{L}_0$ is either an even or odd one. Due to this fact we can study the stability with respect to even (symmetric) and odd (antisymmetric) perturbations separately.

The results of numerical analysis of the discrete spectrum of the linear operator (11) are shown in figure 1. In this figure thick (thin) curves correspond to a stable (unstable) 'one-soliton' solution. The largest autosoliton stability domain lies between the saddle-node bifurcation point S and the Andronov–Hopf bifurcation point H. From our numerical data one can assume the existence of an infinite number of autosoliton stability domains in addition to this domain: each coil of the infinite spiral is supposed to have its own domain. However, since the width of these secondary stability domains rapidly decreases, we have shown only the two largest domains. The second largest stability domain is situated between the saddle-node bifurcation point S′ and the Andronov–Hopf bifurcation point H′. The Andronov–Hopf bifurcations H and H′ correspond to the eigenvectors symmetric under the transformation $x \to -x$. At the saddle-node bifurcation points S and S′ the operator $\hat{L}_0$ has an additional (fourth) zero eigenvalue which corresponds to the adjoint vector $\boldsymbol{\Psi}_4(x) = -\boldsymbol{\Psi}_4(-x) = (\operatorname{Re}\psi_4, \operatorname{Im}\psi_4)^T$, $\psi_4 = (\partial A_0(x,\alpha)/\partial\alpha)_{\alpha=\alpha_s}$, which obeys the relation $\hat{L}_0 \boldsymbol{\Psi}_4(x) = \boldsymbol{\Psi}_2(x)$ [5]. Here $A_0(x, \alpha)$ is the branch of autosoliton solutions defined by the curve shown in figure 1 and $\alpha_s$ is the critical value of the spectral parameter which corresponds to the saddle-node bifurcation point. Note that

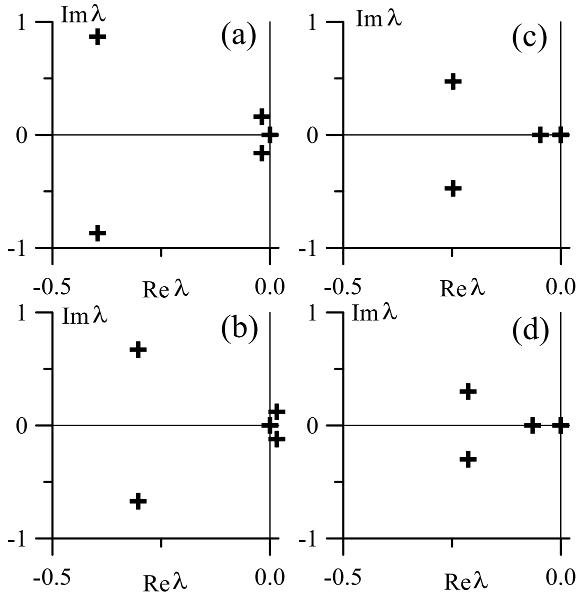


**Figure 3.** Eigenvalues of the operator $\hat{L}_0(x)$ with the largest real parts. $a_0 = 2$ and $\beta = 10$. (*a*) and (*c*) ((*b*) and (*d*)) correspond to $g_0 = 2.08 < g_{0H}$ ($g_0 = 2.10 > g_{0H}$), where $g_0 = g_{0H}$ is the Andronov–Hopf bifurcation point. (*a*) and (*b*) ((*c*) and (*d*)) correspond to even (odd) eigenvectors. Note, that the zero eigenvalue in the left diagrams is doubly degenerate.

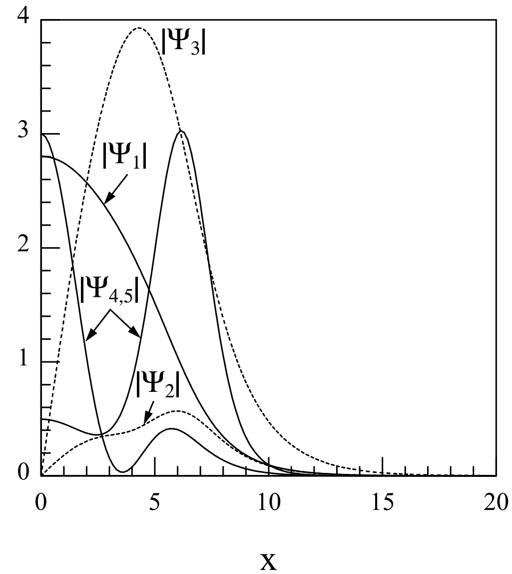


**Figure 4.** Eigenfunctions of the operator $\hat{L}_0(x)$ corresponding to the eigenvalues with largest real parts at the Hopf bifurcation point H. Solid (dashed) curves correspond to even (odd) eigenfunctions. The eigenfunctions $\mathbf{\Psi}_{1,2}$ and the adjoint function $\mathbf{\Psi}_3$ correspond to zero eigenvalues. They are defined by equations (12) and (13), respectively. The eigenfunctions $\mathbf{\Psi}_{4,5}$ correspond to a pair of pure imaginary eigenvalues responsible for the Andronov–Hopf bifurcation.

for the soliton solution of the nonlinear Schrödinger equation one always has four zero eigenvalues [18]. In contrast to this, in our analysis the fourth zero eigenvalue appears only at the saddle-node bifurcation points.

Figure 3 presents several eigenvalues of the operator $\hat{L}_0$ that have the largest real parts. The two upper (lower) graphs correspond to the parameter values below (above) the Andronov–Hopf instability threshold. It follows from this figure that at the Andronov–Hopf bifurcation point a pair of eigenvalues corresponding to even eigenfunctions $\mathbf{\Psi}_{4,5}(x) = \mathbf{\Psi}_{4,5}(-x)$ crosses the imaginary axis. These eigenfunctions are presented in figure 4 together with the eigenfunctions $\mathbf{\Psi}_{1,2}$ and the adjoint function $\mathbf{\Psi}_3$. Note, that according to (12) the square of the modulus of the eigenfunction $\mathbf{\Psi}_1$ coincides with the intensity distribution of the autosoliton solution. Our numerical calculations show that the Andronov–Hopf bifurcation that takes place at the point H is a supercritical one. To the right from this point in figure 1 an oscillating symmetric LS appears (see figure 5).

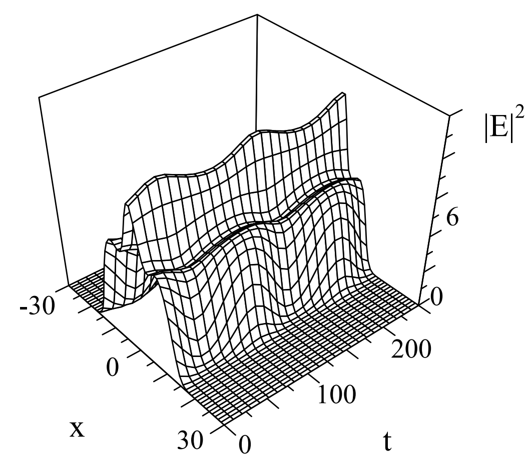


**Figure 5.** Symmetric oscillatory localized structure arising above the Andronov–Hopf bifurcation threshold. $g_0 = 2.102$, $a_0 = 2$, $\beta = 10$, and $\Delta_{1,2} = 0$.

## 5. Computer simulations of 3D laser localized structures

The term ‘laser bullets’ denotes dissipative 3D localized structures of laser radiation. Similar to laser autosolitons (see section 3), they have a discrete spectrum of their characteristics and a hard type of excitation. However, unlike autosolitons, laser bullets are expected to be formed not in a cavity, but in a continuous medium with saturable gain, absorption, and linear frequency dispersion (both normal and anomalous). The laser bullets were predicted in [21] on the basis of an approximate analytical method of moments. Here we present the results of our computer simulations that demonstrate the existence of various types of laser bullets. We restrict our consideration to the case of an inertialess medium and neglect all kinds of frequency detunings. Then, the equation for the field envelope $E$ takes the form

$$\partial_z E - \mathrm{i}\Delta_\perp E - \mathrm{i}D_2\partial_{\tau\tau}E = Ef(|E|^2). \qquad (14)$$

Here $z$ is the longitudinal coordinate, $\Delta_\perp$ is the transverse Laplacian, and $D_2$ is the coefficient of quadratic linear dispersion. The variable $\tau = t - z/v_g$, where $t$ is time, describes the time in the coordinate system moving with group velocity $v_g$. The nonlinear function $f$ is defined by (2) with $\Delta_{1,2} = 0$. The real coefficient in front of the transverse Laplacian has been removed as a result of scaling

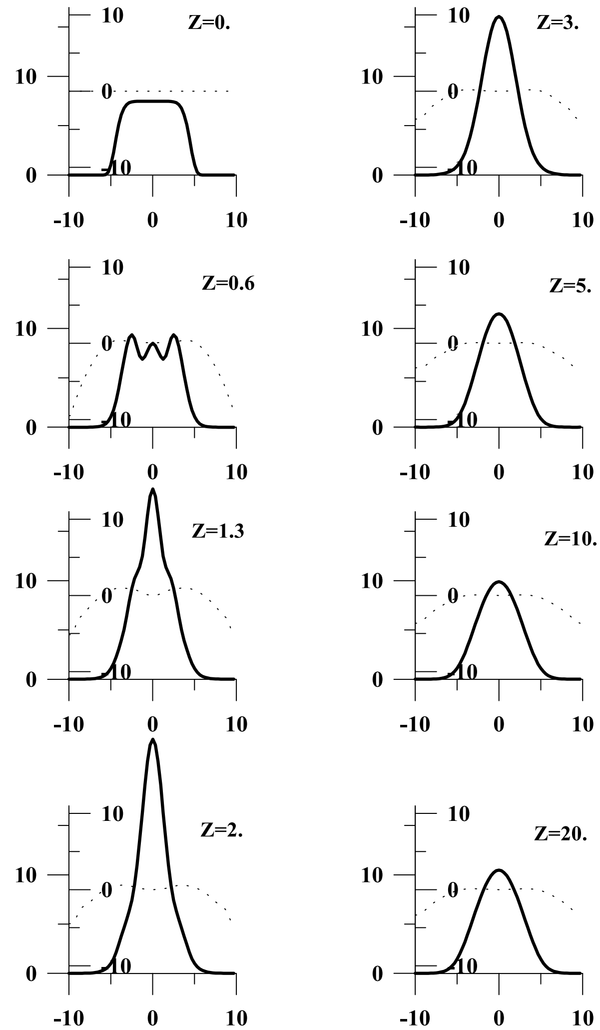


**Figure 6.** Formation of a radially symmetric stationary laser bullet. Intensity (phase) profiles are represented by thick (thin) lines. $g_0 = 2.16$, $a_0 = 2$, $\beta = 10$.

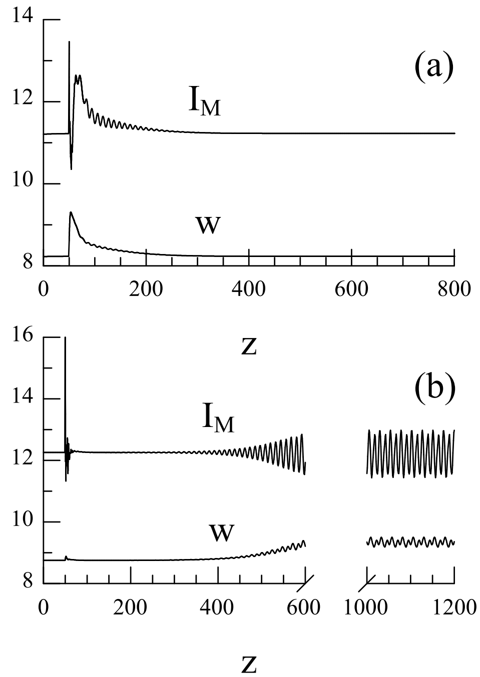


**Figure 7.** Peak intensity $I_M$ and the mean value of intensity distribution width $w$ versus longitudinal coordinate $z$. $a_0 = 2$, $\beta = 10$. Asymmetric perturbation was introduced at $z = 50$. ($a$) $g_0 = 2.154$. Small initial perturbation dissolves in the course of propagation. ($b$) $g_0 = 2.16$. Formation of the oscillating laser bullet.

of transverse coordinates. The scale for the variable $z$ is determined by the value of linear nonresonant absorption. Moreover, we can scale the variable $\tau$ in such a way that $|D_2| = 1$. In our simulations we have used the values $a_0 = 2$ for the linear absorption and $\beta = 10$ for the saturation intensity.

Equation (14) has been solved numerically using the split-step method and the fast Fourier transformation algorithm. The number of spatial harmonics was $64^3$ and $128^3$. The results of our calculations are evidence for the formation of stationary radially symmetric localized intensity distributions for the linear gain parameter $g_0$ in the range from 2.153 to 2.17. If we introduce a sufficiently small asymmetry into the initial field distribution, the symmetry is restored in the course of time evolution. This proves the stability of the stationary symmetric laser bullet. However, if the initial asymmetry exceeds some critical value, a new type of laser bullet can be formed with the field distribution periodic in time and asymmetric in space. Figures 6 and 7 illustrate the process of laser bullet formation. Figure 6 presents transverse intensity and phase distributions evolving in the course of light propagation into a stationary radially symmetric laser bullet. The evolution of the peak intensity and the mean value of the intensity distribution width is shown in Figure 7. Figure 7($a$) (7($b$)) corresponds to the case when initial perturbation introduced at $z = 0$ dissolves (grows) leading to the formation of a stationary (oscillatory) laser bullet. One can see from figure 7($b$) that once the perturbation was introduced, both modulation of maximum intensity and average width of the LS gradually increase and finally are stabilized. Dynamics of the bullet width in the two transverse directions ($x$ and $y$) is approximately antiphase. The periodically oscillating bullets exist in a narrower range of the parameter $g_0$ values than the stationary ones. Thus, in laser systems with energy exchange there can exist stable stationary and oscillating localized structures of radiation with different geometric dimensionality (from $d = 1$ to $d = 3$). For a nonlinear medium with finite population relaxation rates the variety of the localized structures increases.

## 6. Conclusion

Using the bifurcation theory methods we have constructed autosoliton solutions in the model of a bistable laser with one-dimensional transverse section. The autosoliton stability has been studied with the use of combined analytical and numerical methods. It has been shown that the autosoliton solution can exhibit an Andronov–Hopf bifurcation leading to an oscillating LS. Bistable stationary radially symmetric and oscillatory 3D asymmetric localized structures have been found in a saturable dispersive medium which is composed of a mixture of amplifying and absorbing atoms. Numerical evidence of their stability has been presented. In this paper we have considered only the case of inertialess laser media. The results concerning the effect of the finite values of the population relaxation rates on the stability of autosoliton solutions will be presented in a subsequent paper.

## Acknowledgment

This work was supported by the ISTC project no 666.

## References

[1] Rosanov N N and Fedorov S V 1992 *Opt. Spektrosk.* **72** 1394
[2] Rosanov N N, Fedorov A V, Fedorov S V and Khodova G V 1995 *Zh. Eksp. Teor. Fiz.* **107** 376
[3] Rosanov N N 1996 *Progress in Optics* ed E Wolf **35** 1
[4] Rosanov N N 1997 *Optical Bistability and Hysteresis in Distributed Nonlinear Systems* (Moscow: Nauka)
[5] Vladimirov A G, Rosanov N N, Fedorov S V and Khodova G V 1997 *Quantum Electron.* **27** 949
Vladimirov A G, Rosanov N N, Fedorov S V and Khodova G V 1998 *Quantum Electron.* **28** 55
[6] Saffman M, Montgomery D and Anderson D Z 1994 *Opt. Lett.* **19** 518
[7] Slekys D, Staliunas K and Weiss C O 1998 *Opt. Commun.* **149** 113
[8] Taranenko V B, Staliunas K and Weiss C O 1997 *Phys. Rev.* A **56** 1582
[9] Malomed B A 1987 *Physica* D **29** 155
[10] Cross M C and Hohenberg P C 1993 *Rev. Mod. Phys.* **65** 851
[11] Rosanov N N and Khodova G V 1988 *Opt. Spektrosk.* **65** 1399
[12] Rosanov N N, Fedorov A V and Khodova G V 1988 *Phys. Status Solidi* B **150** 545
[13] Rakhmanov A N 1993 *Opt. Spektrosk.* **74** 1184
[14] Rakhmanov A N and Shmalhausen V I 1993 *Proc. SPIE* **2108** 428
[15] Vasil'ev V A, Romanovskii Yu M and Yakhno V G 1979 *Autowave Processes* (Moscow: Nauka)
[16] Kerner B S and Osipov V V 1991 *Autosolitons* (Moscow: Nauka)
[17] Mandel P 1997 *Theoretical Problems in Cavity Nonlinear Optics* (Cambridge: Cambridge University Press)
[18] Buslaev V S and Perel'man G S 1992 *Algebra Anal.* **4** 63
[19] Guckenheimer J and Holmes P 1983 *Nonlinear Oscillations, Dynamical Systems and Bifurcations of Vector Fields* (Springer: Heidelberg)
[20] Arnold V I 1983 *Geometrical Methods in the Theory of Ordinary Differential Equations* (Springer: Heidelberg)
[21] Rosanov N N 1996 *Opt. Spektrosk.* **81** 276